

Left ventricular torsional mechanics in term fetuses and neonates

Olga Patey MD PhD*†‡, Julene S Carvalho MD PhD*†‡§ and Basky Thilaganathan

MD PhD*†§

Molecular & Clinical Sciences Research Institute, St George's University of London*;

Fetal Medicine Unit, St. George's University Hospitals NHS Foundation Trust,

London†;

Brompton Centre for Fetal Cardiology, Royal Brompton Hospital, London‡;

Joint last authors§

Author for correspondence: Dr Olga Patey

Address: Fetal Medicine Unit

4th Floor, Lanesborough Wing

St. George's University Hospitals NHS Foundation Trust

London SW17 0QT

Email: pateyolga@gmail.com

Short title: Perinatal changes in fetal LV torsion

Keywords: fetal heart; left ventricular rotation, twist, and torsion; fetal echocardiography; speckle tracking; perinatal cardiac adaptation

This article has been accepted for publication and undergone full peer review but has not been through the copyediting, typesetting, pagination and proofreading process which may lead to differences between this version and the Version of Record. Please cite this article as doi: [10.1002/uog.20261](https://doi.org/10.1002/uog.20261)

ABSTRACT

Objective Left ventricular (LV) torsion is an important aspect of cardiac mechanics and fundamental to normal ventricular function. The myocardial mechanics of the fetal heart and the transition to extrauterine life have not been explored previously. The aim of this study was to evaluate perinatal changes in LV torsion and its relationship to myocardial function.

Methods A prospective study of 36 women with uncomplicated term pregnancies. Fetal and neonatal conventional, spectral tissue Doppler imaging, and 2D speckle tracking cardiac indices including LV rotation data derived in short axis views at the base and apex of the heart were obtained days before and within hours of birth.

Results There are three patterns of LV twist in term fetuses, from the lowest values of torsion in reversed apex-type ($0.1^\circ/\text{cm}$), through to higher values of infant-type ($1.6^\circ/\text{cm}$) and to the highest values in adult-type LV twist ($4.4^\circ/\text{cm}$). Patterns of fetal LV twist and torsion were also significantly associated with cardiac geometry and functional indices. Perinatal evaluation revealed a significant increase in LV torsion in fetuses exhibiting reversed apex-type LV twist (increased by $2.8^\circ/\text{cm}$, $p=0.01$) and a significant decrease in fetuses with adult-type LV twist (decreased by $3.2^\circ/\text{cm}$, $p=0.008$).

Conclusions This study demonstrates the feasibility of 2D speckle tracking imaging for accurate assessment of rotational cardiac parameters in term fetuses. There are unique perinatal patterns of LV twist that correlate to indices of ventricular geometry and myocardial function. Differences in patterns of LV twist may reflect different

compensatory myocardial adaptation to the physiological environment/loading conditions of late gestation in fetuses and postnatal cardiac adjustment to the acute loading changes that occur at birth.

INTRODUCTION

The fetal heart at term is exposed to significant changes in volume and resistance load due to rapid fetal growth, and as a neonate, to the cardiorespiratory adaptation that occurs at birth. The resultant changes in myocardial performance have been studied in the fetal lamb ^{1,2}, but the extent to which these acute cardiovascular changes influence perinatal cardiac adaptation has been inadequately explored in the human ^{3,4}. Recent advances in cardiac imaging modalities have facilitated an increased interest in rotational mechanics of the heart. Left ventricular (LV) torsion is an important aspect of the cardiac mechanics and fundamental to normal ventricular function. In the adult left ventricle, the opposing rotation of LV apex and base leading to a systolic wringing motion is referred to as a twist, and as torsion when normalised by LV end-diastolic length ^{5,6}. Torsional deformation maximizes storage of potential energy, and the subsequent recoil of twist deformation in diastole is associated with the release of potential energy, augmenting suction and increasing LV diastolic filling ^{7,8}.

Animal data have shown that torsion facilitates uniform distribution of LV stress and fiber shortening across the ventricular wall ⁹. The disappearance of torsion increases endocardial strain and oxygen demand, thereby reducing the efficiency of LV systolic function ^{10,11}. There is growing evidence that LV twist is potentially a superior marker to traditional indices of LV functional assessment in characterizing hemodynamic

aberrations in patients with cardiac pathology^{12,13}. The application of speckle tracking imaging (STI) has permitted a reliable assessment of LV torsional mechanics with reported good reproducibility in the adult population^{14,15}. However, data on assessment of LV rotational mechanics in the fetus¹⁶ and neonate are very limited¹⁷⁻¹⁹. LV torsional mechanics of fetal perinatal adaptation have never been previously explored. Evaluation of perinatal changes in LV torsion and myocardial function may provide insights into perinatal cardiac adaptation in uncomplicated pregnancies at term, and how this is altered in pathological pregnancies.

METHODS

Patients

This was a prospective longitudinal study of 36 women with apparently uncomplicated singleton pregnancies delivering at term. Pregnant women attending for routine antenatal care in the Fetal Medicine Unit at St George's Hospital were recruited if the fetuses had structurally normal hearts and no maternal pre-pregnancy co-morbidities. Exclusion criteria were a fetal structural and chromosomal abnormality, any pregnancy-related complications, and women in labour. All participants gave written informed consents for fetal and neonatal cardiac assessment. The Ethics Committee of NRES Committee London-Surrey Borders approved this research study (REC reference - 12/LO/0945).

Echocardiographic examinations

Conventional echo, spectral tissue Doppler, and 2D speckle tracking imaging (STI) assessments were performed a few days before birth in the fetus and again within hours of birth as a neonate. One investigator (OP) performed all ultrasound examinations using a Vivid E9 ultrasound system (General Electric, Norway). All echocardiographic measurements were performed according to the standardised protocol of the study (see Supplemental methods) and as published previously²⁰⁻²². 2D images for STI analysis were obtained and recorded using the same M5S phased array linear transducer for both fetal and neonatal heart. For fetal STI, four-chamber apical or basal images and short axis views of the heart at the LV basal and apical levels were obtained²³. Due to

advanced gestation and to avoid the rib shadowing, clear short axis views of the fetal heart were easier to obtain scanning from the front of the fetal chest rather than from the back of the fetal chest. Importantly, short axis views were obtained consecutively and not simultaneously²⁴. The basal level of the short axis view was obtained at the level of mitral valve with mitral leaflets visualised, whereas the apical level was defined just proximal to the level with LV lumen obliteration at the end-systolic period, with LV cross-section made as circular as possible. Considering the crucial importance of transducer position/ angulation in the assessment of apical rotation, the most caudal position of the probe was used to exclude the rotational deformation underestimation as previously recommended²⁵. The narrowest possible ultrasound field and a single focal zone were used during image acquisition to obtain frame rates greater than 120 frames per second (fps). Dummy ECG (Lionheart 2 BIO-TEK® Multiparameter Simulator) set at 60 bpm, was used to capture two consecutive fetal cardiac cycles or at least one whole fetal cardiac cycle with a real fetal heart rate of 120-150 bpm. All neonatal examinations were recorded with a simultaneous electrocardiogram. Fetal ECG gating permitted the export of original uncompressed data with *a frame rate of ≥ 120 fps* for off-line analysis on EchoPAC software (version 113, GE Medical System)²⁶. 2D images with the best endocardial border definition were chosen for STI analysis, and in the absence of an ECG, the cardiac cycle was determined using the dummy ECG device, aided by mechanical movements of the atrioventricular valves for basal short-axis views. For the apical short-axis, visualisation of the size of the left ventricle helped in defining the cardiac cycle. The endocardial borders of the myocardium were

manually traced by a point-and-click approach. The software divided the tracking lines into corresponding six myocardial segments (anterior septal, anterior, lateral, posterior, inferior, septal). The region of interest was set at 3-4mm for both fetus and neonate to include the full thickness of the left ventricular segments, thus tracking the net rotation of the myocardium. The software produced the LV torsion curves only if the frame rate of short axis images was the same at LV basal and apical levels. LV net twist was calculated by subtracting the peak basal systolic rotation from the peak apical systolic rotation. LV torsion was calculated as net twist divided by the LV end-diastolic length. Counterclockwise (positive) rotation was recorded as a rotational curve above the baseline, whereas clockwise (negative) rotation was recorded below the baseline. Care was taken to ensure that the direction of the twist was correct for varied fetal orientation according to our proposed study methodology (Supplemental materials, Figures S1 and S2). Briefly, if the heart is scanned from the apex, the STI rotational curves for the counterclockwise positive (+) rotation are conventionally displayed above the baseline and for clockwise negative (-) rotation are below the baseline; whereas if the heart is scanned from the base, the rotation is considered as opposite one (STI curves for counterclockwise (+) rotation are displayed below and for clockwise (-) rotation are above the baseline).

Statistical analysis

Statistical analysis was performed using SPSS version 22.0 (SPSS Inc., Chicago, IL, USA). Both Shapiro-Wilk test and Kolmogorov-Smirnov tests were performed to test

normality. If p -value > 0.05 , the data distribution was considered to be normal. Besides, skewness was examined to determine the normality of the distribution. For normally distributed data, a paired t -test was used to test the null hypothesis that there was no difference in the means between the fetal and neonatal values. Skewed data was assessed with the nonparametric test (Wilcoxon signed rank test). Linear regression analysis was used to examine the relation between rotational parameters and cardiac indices in term fetus and neonate. The differences between measurements were deemed as significant only if the p -values were less than 0.01 (Bonferroni correction for type 1 error or false positive results of multiple measurements). All reported p -values were 2-tailed.

Repeatability and reproducibility

LV rotational measurements of 10 fetal and 10 neonatal echoes were repeated by the same observer (OP) and by two different observers (MB and VDZ) in the same cardiac cycle for calculation of the measurement error, and in a different cardiac cycle for calculation of the overall error (combined acquisition and measurement error). Both, limits of agreement (Lo) with Bland-Altman graphs/Pitman's test of difference in variance, and intra-class correlation coefficient (ICC) were calculated.

RESULTS

A total of 36 women consented to the study, with rotational data available in all neonates and in 25 fetuses due to maternal body habitus and/or unfavorable fetal position in late gestation. The STI mean frame rate for short axis LV at both apical and basal levels was 140 ± 10 fps for fetal heart and 135 ± 11 fps for the neonatal heart. Demographic characteristics and scan details of the pregnancies enrolled in the study are summarized in Table 1. There were no cases of postnatal admission to the NICU / perinatal death.

LV twist in term fetuses

Our finding demonstrated three different patterns of fetal LV twist at term according to directions of apical and basal rotation that corresponded to adult-type (counterclockwise apical and clockwise basal), infant-type (counterclockwise apical and counterclockwise basal) and reversed apex-type (clockwise apical and clockwise basal) configurations (Figures 1, 2 and S3). Reversed apex-type and adult-type LV twist were predominantly produced by basal rotation, whereas infant-type had a preponderance of apical rotation in the generation of differential LV net twist and torsion. Fetal LV torsion was significantly associated with patterns of LV twist (Figure 3A), principally from LV apical rotation compared to LV basal rotation (Figure S4). Linear regression showed a strong correlation of fetal LV torsion with several fetal geometric and functional cardiac indices (Figures 4 and S5, Table 2). Reversed apex-type LV twist had the lowest values of LV torsion and was significantly associated with lowest systolic and diastolic

indices. Adult-type LV twist had the highest values of LV torsion with a strong correlation to indices of increased cardiac function. There was a significant association of LV basal systolic rotation with geometrical cardiac parameters: RV/LV end-diastolic dimension (EDD) ratio and LV sphericity index (Figure 4 C and D). Increased values of RV/LV EDD and reduced LV sphericity were associated with negative basal systolic rotation in the reversed apex-type and adult-type patterns of LV twist.

LV twist in neonates

There were only two patterns of LV twist observed in the neonatal heart in the first hours after birth – infant and adult types (Figures 1, 2 and S3). Neonatal LV torsion was significantly associated with patterns of LV twist (Figure 3B). Both apical and basal systolic rotations contributed equally to LV torsion (Figure S6). Neonatal LV torsion had a strong correlation with several fetal geometric and functional cardiac indices (Figure 5 and Table 2). Adult-type LV twist showed increased LV torsion, RV end-diastolic dimensions, and improved LV systolic and diastolic parameters, whereas infant-type LV twist had lower values of these geometrical and functional parameters. There was no association of LV rotational indices with presence of PDA/ neonatal age at the time of echo assessment.

Perinatal changes in LV twist in term fetuses

Paired comparison of fetal and neonatal rotational parameters demonstrated a convergence of the wide range of LV rotational angles seen in fetuses to a narrower

spread of rotation within the first hours of birth (Figure 6). In fetuses that demonstrated reversed apex-type LV twist, there was a significant increase in neonatal LV apical systolic rotation, whereas fetuses that demonstrated adult-type LV twist exhibited a decrease in neonatal LV basal and apical systolic rotation (Figures 6 and S7, Table 3).

Repeatability and reproducibility

The results of intra- and inter-observer repeatability study with the calculation of limit of agreement (LoA) and intra-class correlation coefficient (ICC) in the same cardiac cycle and a different cardiac cycle are presented in the supplemental Table S1. There was 100% agreement in all cases with regards to patterns of LV twist.

DISCUSSION

This study demonstrates unique patterns of LV twist in term fetuses and notable perinatal changes in LV torsion occurring soon after birth. The specific patterns of LV twist are strongly associated with indices of cardiac geometry and function in term fetuses and neonates suggestive of the compensatory adaptive nature of cardiac mechanics to the physiological loading conditions of late gestation in fetuses and to profound cardiovascular changes that occur soon after birth.

LV rotation, twist and torsion in fetuses at term

Normal fetuses at term exhibited three different patterns of LV twist with the prevalent pattern (46%) being adult-type LV twist associated with the highest values of LV torsion and increased ventricular systolic and improved diastolic function. In contrast, 31% of fetuses showed a unique reversed apex-type LV twist associated with reduced LV and RV functional indices. The interplay of circumferential and longitudinal muscles governs the direction of twist resulting in optimal physiological distribution of LV stress and strain ^{7, 11, 27}. The magnitude of twist is sensitive to ventricular geometry, myocardial contractility and alterations in preload and afterload ^{28, 29}. Only one previous study explored rotational deformation in the fetus and specifically reported decreased of LV torsion with increased gestational age and fetal weight but neglected to report patterns of twist ¹⁶. Our findings of different patterns of LV twist in term fetuses may be explained by cardiac adaptation to increasing loading conditions occurring in the last few weeks of pregnancy where the right ventricle exhibits significant dominance due to

an increased preload and afterload, as a consequence, RV chamber dilatation, while the left ventricle faces with reduced loading conditions ²⁰.

Adult and paediatric studies have demonstrated that increased loading conditions influence RV dimensions and subsequently interventricular subepicardial fiber continuity at the region of fibrous trigone thereby affecting LV twist ³⁰⁻³². Similarly, our data suggests that in the fetus, the increased RV dimensions and a less globular left ventricle are correlated with an increased negative clockwise basal rotation in both adult-type and reversed apex-type patterns of the LV twist. Adult-type LV twist was associated with the increased ventricular functional parameters and the highest values of LV torsion, but in contrast, reversed apex-type LV twist had the lowest values of apical circumferential strain rate, LV ejection time, and the lowest indices of RV systolic and diastolic function. Notably, the same reversed apex-type pattern of LV twist (rigid or solid body rotation) with near absent twist, has been reported in cases of LV non-compaction cardiomyopathy and other cardiac pathologies ^{33, 34}. We speculate that specific patterns of LV twist exhibited by fetuses may serve as a potential marker of subclinical myocardial dysfunction.

LV rotation, twist, and torsion in neonates

Comparison of paired perinatal data demonstrated a wide range of LV torsional values in fetuses change to a narrower range of rotational angles in the neonate. Postnatally, neonates demonstrated only two patterns of rotation with predominantly an infant-type LV twist pattern. An adult-type LV twist pattern was seen in 35% of neonates and

associated with increased LV torsion, LV systolic/diastolic function and greater RV end-diastolic dimensions. These findings suggest a compensatory phenotype for adult-type LV twist in the presence of more globular right ventricle in newborns. The findings of two rotational patterns in neonates are in agreement with several other STI studies, which included normal infants and children^{17, 35-37}. The notable postnatal changes in the patterns of LV rotation are likely to be a consequence of profound alterations in loading conditions occurring with birth impacting cardiac geometry and function²⁰. Animal studies^{38,39} showed that fetal myocardium plasticity is much higher than postnatal due to the expression of a particular isoform of titin. Rapid switch from the fetal compliant N2BA subtype of titin to the stiffer neonatal N2B isoform was claimed to have a major role in the perinatal cardiac adaptation to loading conditions⁴⁰. The effect of acute changes in loading conditions, heart rate and contractility on the torsional deformation in normal heart remain controversial^{28, 29, 41, 42}. The marked decrease in neonatal RV size might contribute to rotation of the base of the heart in the same counterclockwise direction with the resultant change in LV twist patterns leading to dominance of infant-type pattern LV twist. Our postnatal findings of a strong correlation of increased LV torsion with increased LV basal/apical circumferential myocardial deformation and decreased LV longitudinal contractility supports this hypothesis. The persistence of a more globular right ventricle in the minority of normal fetuses after birth is associated with persistence of adult-type pattern LV twist, also consistent with this supposition.

Study strengths and limitations

The main strength of the present study is its prospective follow-up design, where the impact of a natural intervention could be studied longitudinally from fetus to neonate. By restricting the study to term pregnancies and fetuses of normal size, we reduced the effect of confounding variables on torsional mechanics. Rotational data was available in 25 of 36 term fetuses, but despite this limitation, the quality of obtained for STI analysis short axis images was adequate for feasible and reproducible assessment of myocardial deformation according to the developed study protocol. The image acquisition was conducted in the same manner and with the same ultrasound transducer in both fetal and neonatal groups. Before standardization of software algorithm across different manufacturers, the inter-vendor discordance of fetal and neonatal speckle tracking parameters should be considered so that the actual rotational values measured might not be replicated on other ultrasound systems. Additionally, dummy ECG, mitral valve motion, and visualization of size of the left ventricle in the short axis view have been used as surrogates for defining the cardiac cycle.

Conclusions

The study findings demonstrate the feasibility of 2D speckle tracking imaging for assessment of rotational cardiac parameters in normal term fetuses. There are unique perinatal patterns of LV twist that correlate to indices of ventricular geometry, myocardial performance, and cardiac function. Differences in patterns of LV twist may reflect different compensatory myocardial adaptation to the physiological

environment/loading conditions of late gestation in fetuses and postnatal cardiac adjustments to the acute perinatal loading changes in neonates.

Clinical perspectives

The proposed methodology for evaluation of perinatal LV torsional mechanics provides a novel approach for the characterization of myocardial performance. The assessment of a specific pattern of LV twist as a diagnostic marker of subclinical changes in fetal and neonatal myocardial performance might have the potential applicability in understanding of fetal cardiac adaptation in pregnancies complicated by different pathologies such as fetal growth restriction, maternal diabetes and congenital heart defect. Any observed alterations in myocardial function in these fetal conditions may also have an influence on offspring cardiovascular health.

ACKNOWLEDGEMENTS

We are grateful to General Electric (GE) Ultrasound Company for providing Vivid E9 ultrasound platform and EchoPAC software for this research. We also thank Dr Margarita Bartsota and Miss Vahideh Davatgar Zahiri for helping with echo measurements for inter-observer reproducibility study and all sonographers, midwives and doctors of the Fetal Medicine Unit, St George's Hospital for their contribution in the patient's recruitment.

FUNDING SOURCES

OP was partly supported by Children's Heart Unit Fund (CHUF), Royal Brompton and Harefield Hospital Charity [registered no. 1053584] and by SPARKS Charity (registered no.1003825, grant ref. no.14EDI01).

REFERENCES

1. Teitel DF, Dalinghaus M, Cassidy SC, Payne BD, Rudolph AM. In utero ventilation augments the left ventricular response to isoproterenol and volume loading in fetal sheep. *Pediatr Res*. 1991; **29**: 466-472.
2. Rudolph AM. Distribution and regulation of blood flow in the fetal and neonatal lamb. *Circ Res*. 1985; **57**: 811-821.
3. Iwashima S, Sekii K, Ishikawa T, Itou H. Serial change in myocardial tissue Doppler imaging from fetus to neonate. *Early Hum Dev*. 2013; **89**: 687-692.
4. Maskatia SA, Pignatelli RH, Ayres NA, Altman CA, Sangi-Haghpeykar H, Lee W. Longitudinal Changes and Interobserver Variability of Systolic Myocardial Deformation Values in a Prospective Cohort of Healthy Fetuses across Gestation and after Delivery. *J Am Soc Echocardiogr*. 2016; **29**: 341-349.
5. Buckberg G, Hoffman JI, Mahajan A, Saleh S, Coghlan C. Cardiac mechanics revisited: the relationship of cardiac architecture to ventricular function. *Circulation*. 2008; **118**: 2571-2587.
6. Young AA, Cowan BR. Evaluation of left ventricular torsion by cardiovascular magnetic resonance. *J Cardiovasc Magn Reson*. 2012; **14**: 49.
7. Taber LA, Yang M, Podszus WW. Mechanics of ventricular torsion. *J Biomech*. 1996; **29**: 745-752.
8. Sengupta PP, Tajik AJ, Chandrasekaran K, Khandheria BK. Twist mechanics of the left ventricle: principles and application. *JACC Cardiovasc Imaging*. 2008; **1**: 366-376.

9. Arts T, Veenstra PC, Reneman RS. Epicardial deformation and left ventricular wall mechanisms during ejection in the dog. *Am J Physiol*. 1982; **243**: H379-390.
10. Beyar R, Sideman S. Left ventricular mechanics related to the local distribution of oxygen demand throughout the wall. *Circ Res*. 1986; **58**: 664-677.
11. Sengupta PP, Khandheria BK, Narula J. Twist and untwist mechanics of the left ventricle. *Heart Fail Clin*. 2008; **4**: 315-324.
12. Bell SP, Nyland L, Tischler MD, McNabb M, Granzier H, LeWinter MM. Alterations in the determinants of diastolic suction during pacing tachycardia. *Circ Res*. 2000; **87**: 235-240.
13. Bertini M, Sengupta PP, Nucifora G, Delgado V, Ng AC, Marsan NA, Shanks M, van Bommel RJ, Schalij MJ, Narula J, Bax JJ. Role of left ventricular twist mechanics in the assessment of cardiac dyssynchrony in heart failure. *JACC Cardiovasc Imaging*. 2009; **2**: 1425-1435.
14. Park CM, March K, Williams S, Kukadia S, Ghosh AK, Jones S, Tillin T, Chaturvedi N, Hughes AD. Feasibility and reproducibility of left ventricular rotation by speckle tracking echocardiography in elderly individuals and the impact of different software. *PLoS One*. 2013; **8**: e75098.
15. Stewart GM, Yamada A, Kavanagh JJ, Haseler LJ, Chan J, Sabapathy S. Reproducibility of Echocardiograph-Derived Multilevel Left Ventricular Apical Twist Mechanics. *Echocardiography*. 2016; **33**: 257-263.

16. Li LC, M.; Hsu, H.H; Zhang, M., Klas, B.; Danford, D.A.; Kutty, S. Left Ventricular Rotational and Twist Mechanics in the Human Fetal Heart. *J Am Soc Echocardiogr.* 2017; **30**: 773-780.
17. Al-Naami GH. Torsion of young hearts: a speckle tracking study of normal infants, children, and adolescents. *Eur J Echocardiogr.* 2010; **11**: 853-862.
18. Zhang Y, Zhou QC, Pu DR, Zou L, Tan Y. Differences in left ventricular twist related to age: speckle tracking echocardiographic data for healthy volunteers from neonate to age 70 years. *Echocardiography.* 2010; **27**: 1205-1210.
19. Laser KT, Hauffe P, Haas NA, Korperich H, Faber L, Peters B, Fischer M, Kececioglu D. Percentiles for left ventricular rotation: comparison of reference values to paediatric patients with pacemaker-induced dyssynchrony. *Eur Heart J Cardiovasc Imaging.* 2014; **15**: 1101-1107.
20. Patey O, Gatzoulis MA, Thilaganathan B, Carvalho JS. Perinatal Changes in Fetal Ventricular Geometry, Myocardial Performance, and Cardiac Function in Normal Term Pregnancies. *J Am Soc Echocardiogr.* 2017; **30**: 485-492.e485.
21. Patey O, Carvalho, J.S., Thilaganathan, B. Perinatal changes in cardiac geometry and function in growth restricted fetuses at term. *Ultrasound Obstet Gynecol.* 2018 (in press).
22. Patey O, Carvalho, J.S., Thilaganathan, B. Perinatal changes in fetal cardiac geometry and function in gestational diabetic pregnancies at term. *Ultrasound in Obstetrics and Gynecology.* 2018 (in press).

23. Park SJ, Miyazaki C, Bruce CJ, Ommen S, Miller FA, Oh JK. Left ventricular torsion by two-dimensional speckle tracking echocardiography in patients with diastolic dysfunction and normal ejection fraction. *J Am Soc Echocardiogr.* 2008; **21**: 1129-1137.
24. Enzensberger C, Degenhardt J, Tenzer A, Doelle A, Axt-Flidner R. First experience with three-dimensional speckle tracking (3D wall motion tracking) in fetal echocardiography. *Ultraschall Med.* 2014; **35**: 566-572.
25. van Dalen BM, Vletter WB, Soliman OI, ten Cate FJ, Geleijnse ML. Importance of transducer position in the assessment of apical rotation by speckle tracking echocardiography. *J Am Soc Echocardiogr.* 2008; **21**: 895-898.
26. Germanakis I, Gardiner H. Assessment of fetal myocardial deformation using speckle tracking techniques. *Fetal Diagn Ther.* 2012; **32**: 39-46.
27. Omar AM, Vallabhajosyula S, Sengupta PP. Left ventricular twist and torsion: research observations and clinical applications. *Circ Cardiovasc Imaging.* 2015; **8**.
28. Park SJ, Nishimura RA, Borlaug BA, Sorajja P, Oh JK. The effect of loading alterations on left ventricular torsion: a simultaneous catheterization and two-dimensional speckle tracking echocardiographic study. *Eur J Echocardiogr.* 2010; **11**: 770-777.
29. Laser KT, Haas NA, Jansen N, Schaffler R, Palacios Argueta JR, Zittermann A, Peters B, Korperich H, Kececioglu D. Is torsion a suitable echocardiographic parameter to detect acute changes in left ventricular afterload in children? *J Am Soc Echocardiogr.* 2009; **22**: 1121-1128.

30. Cheung YF, Wong SJ, Liang XC, Cheung EW. Torsional mechanics of the left ventricle in patients after surgical repair of tetralogy of Fallot. *Circ J*. 2011; **75**: 1735-1741.
31. Molano LC, Viacroze, C., Gounane, C., Cuvelier, A., Muir, J.F. Left ventricular systolic torsion is decreased due to right ventricular dilatation in pulmonary hypertension patients. American Thoracic Society International Conference. 2016.
32. Dufva MJ, Truong, U., Shandas, R., Kheyfets, V. Left Ventricular torsion rates by CMR correlate with invasively-derived hemodynamic data in pediatric pulmonary hypertension. *J Cardiovasc Magn Reson*. 2016; **18** (Suppl 1):P4.
33. Peters F, Khandheria BK, Libhaber E, Maharaj N, Dos Santos C, Matioda H, Essop MR. Left ventricular twist in left ventricular noncompaction. *Eur Heart J Cardiovasc Imaging*. 2014; **15**: 48-55.
34. van Dalen BM, Caliskan K, Soliman OI, Kauer F, van der Zwaan HB, Vletter WB, van Vark LC, Ten Cate FJ, Geleijnse ML. Diagnostic value of rigid body rotation in noncompaction cardiomyopathy. *J Am Soc Echocardiogr*. 2011; **24**: 548-555.
35. Notomi Y, Srinath G, Shiota T, Martin-Miklovic MG, Beachler L, Howell K, Oryszak SJ, Deserranno DG, Freed AD, Greenberg NL, Younoszai A, Thomas JD. Maturational and adaptive modulation of left ventricular torsional biomechanics: Doppler tissue imaging observation from infancy to adulthood. *Circulation*. 2006; **113**: 2534-2541.

36. Takeuchi M, Nakai H, Kokumai M, Nishikage T, Otani S, Lang RM. Age-related changes in left ventricular twist assessed by two-dimensional speckle-tracking imaging. *J Am Soc Echocardiogr.* 2006; **19**: 1077-1084.
37. James A, Corcoran JD, Mertens L, Franklin O, El-Khuffash A. Left Ventricular Rotational Mechanics in Preterm Infants Less Than 29 Weeks' Gestation over the First Week after Birth. *J Am Soc Echocardiogr.* 2015; **28**: 808-817.e801.
38. Opitz CA, Leake MC, Makarenko I, Benes V, Linke WA. Developmentally regulated switching of titin size alters myofibrillar stiffness in the perinatal heart. *Circ Res.* 2004; **94**: 967-975.
39. Walker JS, de Tombe PP. Titin and the developing heart. *Circ Res.* 2004; **94**: 860-862.
40. Lahmers S, Wu Y, Call DR, Labeit S, Granzier H. Developmental control of titin isoform expression and passive stiffness in fetal and neonatal myocardium. *Circ Res.* 2004; **94**: 505-513.
41. Dong SJ, Hees PS, Huang WM, Buffer SA, Jr., Weiss JL, Shapiro EP. Independent effects of preload, afterload, and contractility on left ventricular torsion. *Am J Physiol.* 1999; **277**: H1053-1060.
42. Gibbons Kroeker CA, Tyberg JV, Beyar R. Effects of load manipulations, heart rate, and contractility on left ventricular apical rotation. An experimental study in anesthetized dogs. *Circulation.* 1995; **92**: 130-141.

FIGURE LEGENDS

Figure 1 Cardiac mechanics of different LV twist patterns in term fetus. Influence of LV and RV geometry on balance between subepicardial rotation (R1) and subendocardial rotation (R2) in the production of (A) adult-type, (B) infant-type and (C) reversed apex-type LV twist in term fetus.

Figure 2 Distribution of LV twist patterns in term fetus and neonate. Bar charts demonstrate distribution and perinatal changes in patterns of LV twist in normal term fetuses: three patterns of LV twist (adult-type, infant-type and reversed apex type) in term fetus change to two patterns (infant-type and adult-type) in neonates. Fetuses are shown *in black*; neonates are *in white* color.

Figure 3 Variability of LV torsion across LV twist patterns in term fetuses and neonates. Scatter plot demonstrating significant differences ($p < 0.0001$) in LV torsion median values between different patterns of LV twist in (A) normal fetuses at term and (B) normal neonates. Reversed apex-type LV twist is shown *in white circles*, infant-type is *in gray squares*, and adult-type is *in black diamonds*.


Figure 4 Significant associations of LV rotational parameters with cardiac geometrical and functional indices in term fetuses. Linear regression scatter plots show a significant association of fetal LV torsion with (A) RV E/E' ratio ($p < 0.0001$, $R^2 = 0.72$), (B) LV ejection time normalised by cardiac cycle length ($p = 0.004$, $R^2 = 0.41$),

and LV basal rotation with (C) RV/LV end-diastolic dimension (EDD) ratio ($p < 0.0001$, $R^2 = 0.66$) and (D) LV sphericity index ($p < 0.0001$, $R^2 = 0.60$). Sphericity index = ventricular EDD/ ventricular end-diastolic length. Reversed apex-type LV twist is shown *in white circles*, infant-type is *in gray squares*, and adult-type is *in black diamonds*.

Figure 5 Significant association of LV torsion with cardiac geometrical and functional indices in neonates. Linear regression scatter plots show a significant association of neonatal LV torsion with: (A) RV/LV end-diastolic dimension ratio (EDD) ($p = 0.002$, $R^2 = 0.42$), (B) LV apical systolic circumferential strain rate (C-SR) ($p < 0.0001$, $R^2 = 0.58$), (C) LV basal early diastolic C-SR ($p = 0.006$, $R^2 = 0.74$), (D) LV isovolumetric relaxation time' (IVRT') normalised by cardiac cycle length ($p = 0.001$, $R^2 = 0.72$). Infant-type is *in gray squares*, and adult-type is *in black diamonds*.

Figure 6 Perinatal changes in LV torsion from fetus to neonate. The linear plot of perinatal changes in LV torsion from all normal fetuses to respective neonates demonstrates a wide range of torsional values in fetal hearts converging to the narrower spread of torsional range in neonates. Reversed-type LV twist is shown *in red*, infant-type is *in yellow*, and adult-type is *in green*.

Figure S1 Position of the fetus on the ultrasound screen for identification of the fetal LV rotational direction. If the fetal position on the screen corresponds to the usual adult/paediatric position for LV short axis acquisition, assuming that the *marker is on the right side* of the ultrasound machine screen, the interpretation of rotational direction from STI rotational curves should be conventionally regarded as positive counter-clockwise rotation when these curves are displayed above the baseline, and considered as negative clockwise one for the rotational curves shown below the baseline (A); If the fetal orientation on the screen is opposite to the adult/paediatric position, the direction of rotation produced by speckle tracking imaging should be interpreted as the opposite one: rotation is regarded as positive counter-clockwise when the rotational deformational curves displayed below the baseline, and negative clockwise rotation for rotational curves shown above the baseline (B).

Figure S2 Various fetal positions and transducer orientations for the short axis image acquisition with corresponding short axis images on the ultrasound screen and directions of the LV rotation. The LV rotational direction is regarded as conventional - counterclockwise (+) with rotational curves displayed above the baseline and clockwise (-) with rotational curved shown below the baseline - when fetus is in the positions A, B, C, D. The LV rotational direction is changed to the opposite one - counterclockwise (+) when rotational curves displayed below the baseline and clockwise (-) with rotational curves shown above the baseline - when fetus is in the positions E, F, G, H. RV, right ventricle; LV, left ventricle; MV, mitral valve; , a

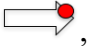

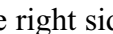
transducer with a red dot marker showing the position and orientation of the ultrasound probe on the fetal chest for acquiring a short axis view of the fetal heart; , a transducer position with a red dot marker corresponding to the scanning from the front of the chest; , a marker on the right side of the ultrasound screen; , scanning plane.

Figure S3 Patterns of LV twist in normal term fetus and neonate. Reversed apex-type LV twist (*in white colour*) showed the clockwise direction of both the apex and the base; infant-type (*in grey colour*) had the counter clockwise rotation of both the apex and the base; adult-type (*in black colour*) demonstrated the counter clockwise rotation of the apex and clockwise rotation of the base.

Figure S4 Association of apical and basal rotation with LV torsion in term fetuses. Scatter plots demonstrating (A) significant linear correlation of LV torsion with the apical systolic rotation ($p < 0.0001$, $R^2 = 0.66$), and (B) no association of LV torsion with the LV basal systolic rotation in the normal term fetus ($p = 0.430$). Reversed apex-type LV twist is shown *in white circles*, infant-type is *in grey squares*, and adult-type is *in black diamonds*.

Figure S5 Significant associations of LV torsion with additional cardiac functional indices in term fetuses. Linear regression scatter plots show a significant association of fetal LV torsion with (A) RV global longitudinal myocardial diastolic velocity ratio

e'/a' (p=0.001, R²=0.45), (B) RV myocardial performance index' (MPI') (p=0.001, R²=0.52), (C) LV apical systolic circumferential strain rate (C-SR) (p=0.003, R²=0.51), and (D) RV longitudinal strain rate (L-SR) diastolic ratio (p =0.010, R²=0.43). Reversed apex-type LV twist is shown *in white circles*, infant-type is *in grey squares*, and adult-type is *in black diamonds*.

Figure S6 Association of apical and basal rotation with LV torsion in neonates.

Scatter plots demonstrating a significant linear correlation of LV torsion with (A) apical (p<0.0001, R²=0.69) and (B) basal systolic rotation (p<0.0001, R²=0.83) in the normal neonate. Infant-type is *in grey squares*, and adult-type is *in black diamonds*.

Figure S7 Speckle tracking imaging (STI) demonstrates LV basal and apical rotation and LV twist in the term fetus and neonate.

Segmental STI curves at the basal (A) and apical (B) levels, and the resulting LV twist curve (C) in the term fetus. The segmental basal (D), apical (E) and the resulting twist (F) STI curves in the neonate (*the same baby 22 hours after birth*). The fetus revealed Adult-type LV twist with counterclockwise apical rotation and clockwise basal rotation. The direction of the LV twist was adjusted with respect to fetal orientation (cephalic position) on the ultrasound screen as the heart was viewed from the base. The neonate showed Infant-type LV twist with clockwise rotation of the apex and base. AVC, aortic valve closure; green dash vertical line denotes the AVC; yellow dash vertical lines mark the beginning and the end of the cardiac cycle.

Table 1 Demographic characteristic of the study population

Parameter	Characteristics
<i>Maternal characteristics</i>	
Maternal age (years)	33 (31-35)
Ethnicity (number): Caucasian	27 (68%)
Asian	9 (23%)
Afro-Caribbean	4 (10%)
Delivery mode (C-section) (number)	7 (18%)
<i>Fetal cardiac assessment</i>	
Gestational age (weeks)	39 (38-39)
Time gap between the fetal scan and birth (days)	7 (4-13)
Fetal heart rate (beats per minute)	139 ± 11
<i>Neonatal cardiac assessment</i>	
Neonate's age at the time of scan (hours)	15 (10-23)
Neonate's sex (male) (number)	19 (53%)
Neonate's weight (kilograms)	3.48 ± 0.47
Small PFO presence (number)	36 (100%)
Small PDA presence (number)	29 (81%)
Tricuspid regurgitation presence (number)	3 (8%)
Neonatal heart rate (beats per minute)	114 ± 14

Values are mean ± SD, median (interquartile range), or n (%), PFO, patent foramen ovale; PDA, patent ductus arteriosus.

Table 2 Linear regression analysis of LV torsion with other cardiac indices derived by different ultrasound techniques in term fetuses and neonates

LV rotational parameters	Cardiac geometric and functional parameters	US modality	R ²	P
<i>Term fetuses</i>				
LV basal Rot, °	RV/LV EDD ratio	B-mode (2D)	0.66	<0.0001
	LV sphericity index	B-mode (2D)	0.60	<0.0001
LV torsion, °/cm	LV global apical Rot, °	short axis STI	0.66	<0.0001
	LV global apical C-SR, 1/s	short axis STI	0.32	0.017
	LV ET', s	PW Doppler	0.41	0.006
	MAPSE, mm	M-mode	0.37	0.010
	RV global L-V e'/a', cm/s	4ch view- STI	0.36	0.006
	RV MPI'	PW-TDI	0.48	0.004
	RV E/E'	PW-TDI	0.72	0.001
	RV global L-SR e/a	4ch view- STI	0.29	0.040
	RV ET', s	PW-TDI	0.36	0.032
	<i>Neonates</i>			
LV torsion, °/cm	RV/LV EDD ratio	B-mode (2D)	0.42	0.002
	LV global apical Rot, °	short axis STI	0.69	<0.0001
	LV global basal Rot, °	short axis STI	0.83	<0.0001

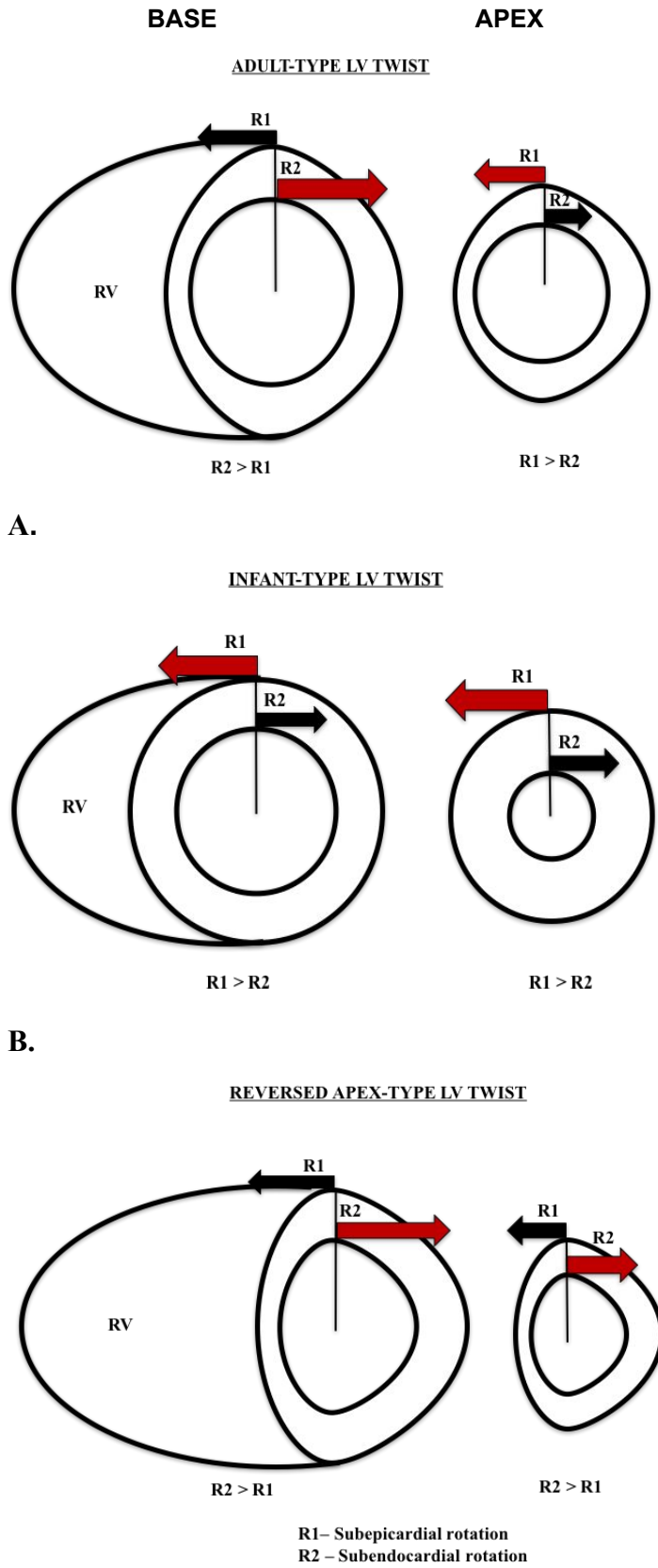
LV global apical C-S, %	short axis STI	0.62	0.001
LV global apical C-SR, 1/s	short axis STI	0.58	<0.0001
LV global apical C-SR e, 1/s	short axis STI	0.55	0.006
LV global basal C-S, %	short axis STI	0.35	0.031
LV global basal C-SR, 1/s	short axis STI	0.26	0.023
LV global basal C-SR e, 1/s	short axis STI	0.74	0.006
LV IVRT, s	PW Doppler	0.72	0.001
MAPSE, mm	M-mode	0.39	0.021

US, ultrasound; STI, speckle tracking imaging; PW-TDI, pulsed wave tissue Doppler imaging; LV, left ventricular; RV, right ventricular; ; Rot, systolic rotation; C-S, circumferential strain; C-SR, circumferential systolic strain rate; C-SR e, circumferential early diastolic strain rate; L-SR, longitudinal strain rate; L-V, longitudinal myocardial systolic velocities; EDD, end-diastolic dimension; ET', ejection time; MPI, myocardial performance index; E/E', diastolic ratio of transvalvar early diastolic filling obtained by PW Doppler and myocardial early diastolic filling obtained by PW-TDI; IVRT, isovolumetric relaxation time; MAPSE, mitral annular plane systolic excursion; °, degrees.

Table 3 Perinatal changes in LV rotation, twist, and torsion in fetuses at term

Parameter	Fetal	Neonatal	P
<i>Fetal Pattern 1 LV twist</i>			
LV basal global systolic rotation, °	-5.13 (6.50)	-4.14 (8.35)	0.090
LV apical global systolic rotation, °	0.04 (4.25)	7.12 (2.18)	<0.0001
LV net twist, °	0.36 (8.48)	10.80 (11.83)	0.008
LV torsion, °/cm	0.11 (3.17)	2.90 (3.72)	0.013
<i>Fetal Pattern 2 LV twist</i>			
LV basal global systolic rotation, °	3.46 (4.93)	0.54 (10.85)	0.133
LV apical global systolic rotation, °	7.41 (4.46)	5.82 (2.85)	0.075
LV net twist, °	4.22 (7.71)	6.42 (13.62)	0.781
LV torsion, °/cm	1.60 (2.0)	2.0 (4.2)	0.982
<i>Fetal Pattern 3 LV twist</i>			
LV basal global systolic rotation, °	-4.49 (4.72)	-1.54 (6.81)	0.015
LV apical global systolic rotation, °	8.32 ± 1.63	5.03 ± 0.59	0.001
LV net twist, °	13.98 ± 3.32	5.32 ± 3.45	<0.0001
LV torsion, °/cm	4.40 (2.00)	1.20 (2.0)	0.008

Values are mean ± SD, median (interquartile range), or n (%); LV, left ventricular; RV, right ventricular; °, degrees.



C.

Figure 1.

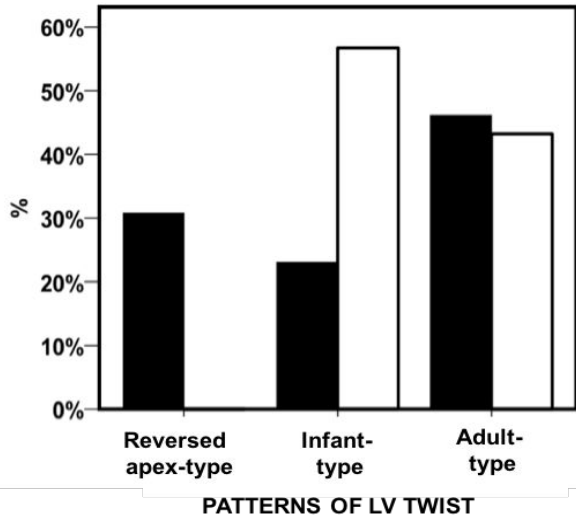
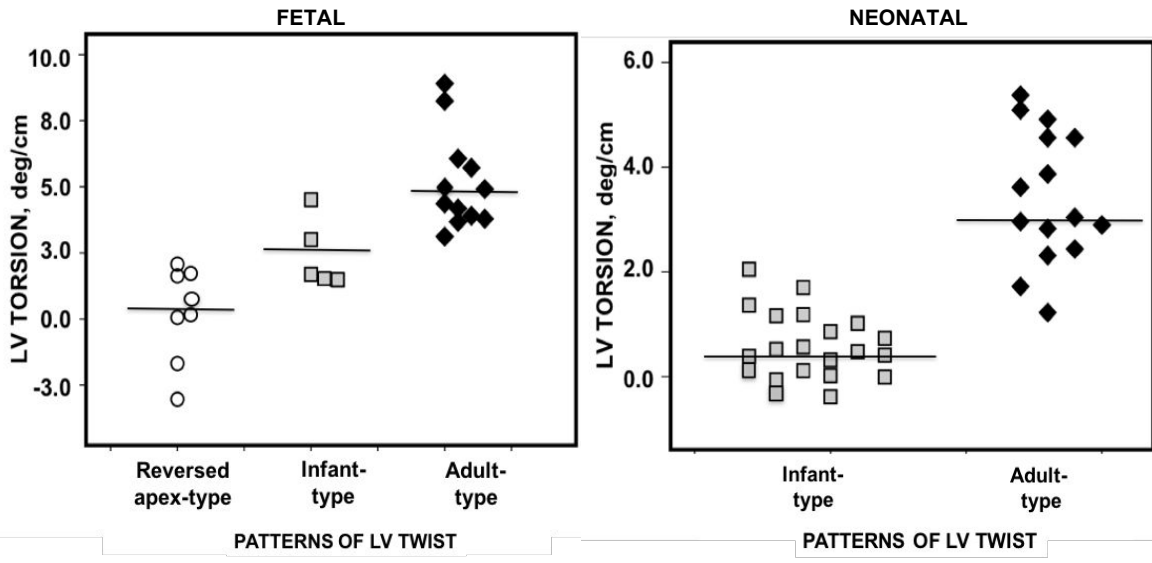


Figure 2.



A.

B.

Figure 3.

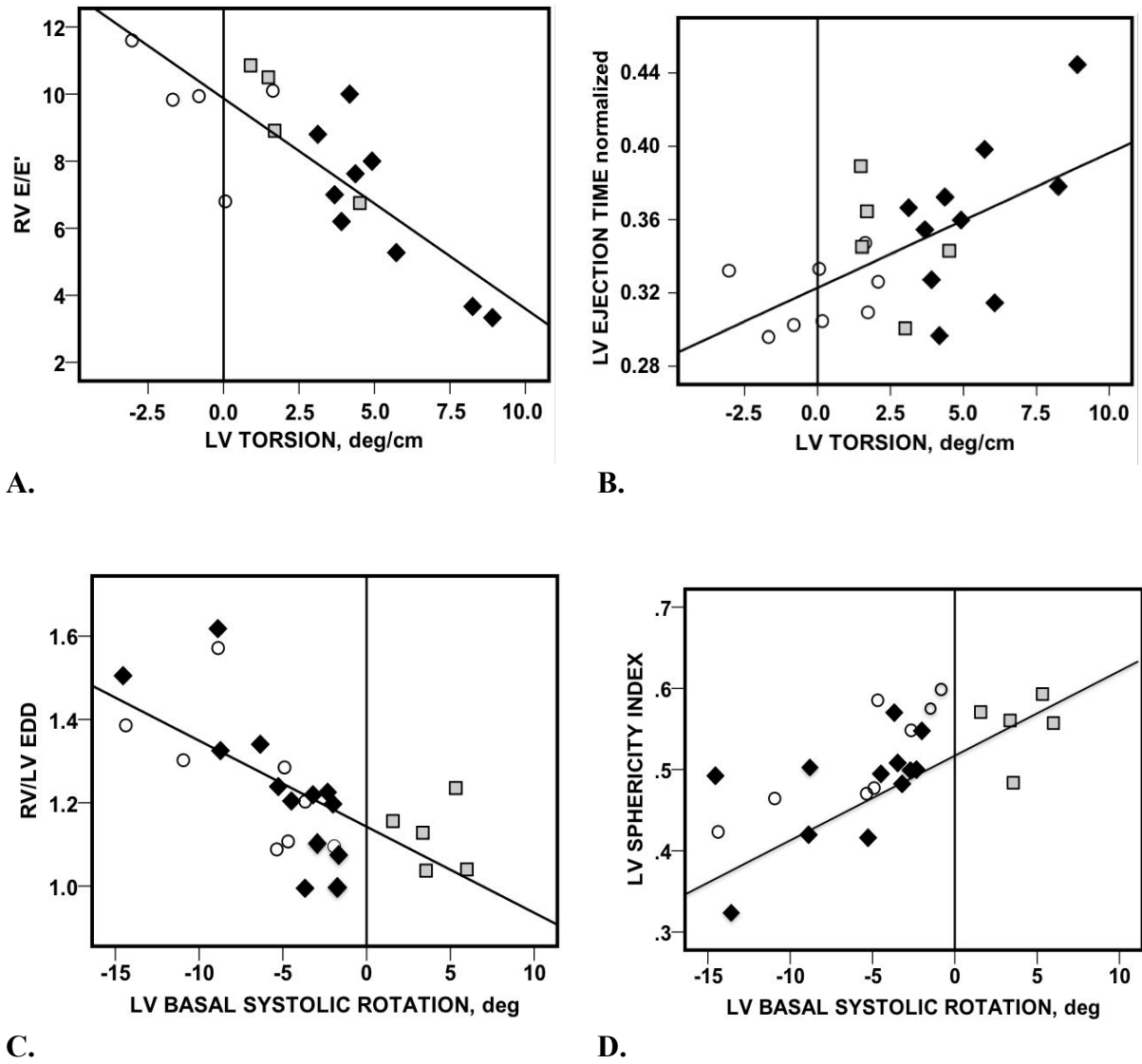


Figure 4.

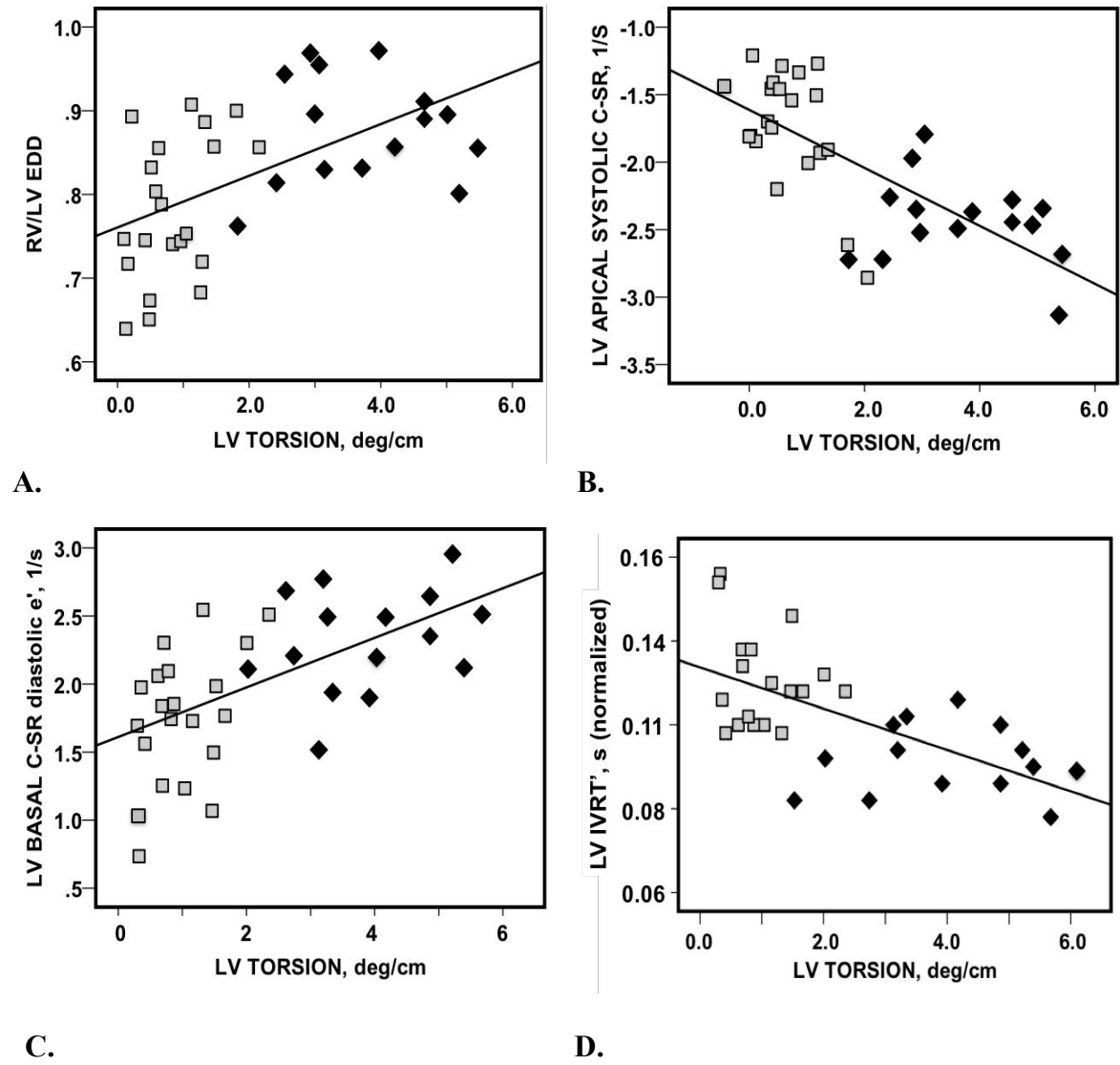


Figure 5.

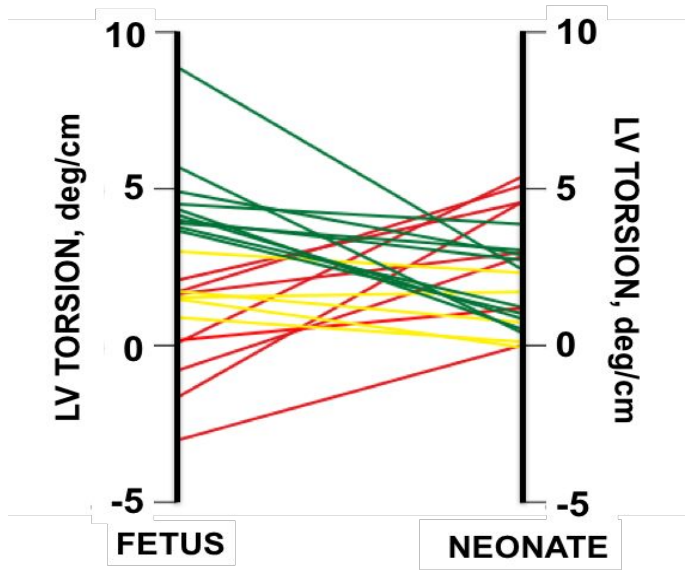


Figure 6.